

# Resonance Behavior of Buried Land Mines

Christoph T. Schröder and Waymond R. Scott, Jr.

School of Electrical and Computer Engineering  
Georgia Institute of Technology  
Atlanta, GA 30332-0250  
USA

## ABSTRACT

A three-dimensional finite-difference time-domain model for elastic waves in the ground has been developed and implemented on a massively parallel computer. The numerical model has been developed as part of a project in which elastic and electromagnetic waves are used synergistically to detect buried land mines. The numerical model is used to study the interaction of elastic waves with buried land mines. As a first approach, a simple model for a TS-50 antipersonnel mine has been developed, and the interaction of elastic waves with the buried mine has been investigated. In both experimental results and numerical simulations, resonant oscillations occur at the location of the buried mine. To further explore the resonant behavior of a buried land mine, a refined mine model has been developed that includes more details of the actual mine. Using the refined mine model, the nature of the resonance is explained, and the parts of the mine that influence the resonant oscillations are identified. Results are presented which describe the resonance as a function of burial depth and soil parameters.

**Keywords:** land mine, elastic, acoustic, FDTD, finite-difference, resonance

## 1. INTRODUCTION

At the Georgia Institute of Technology, a system is being developed in which buried land mines are located by using both elastic (acoustic) and electromagnetic waves.<sup>1,2</sup> In this system, elastic waves are excited that interact with a buried land mine. The waves cause the mine and the surface above the mine to vibrate. An electromagnetic radar records the vibrations and, thus, detects the mine. To investigate the characteristics of elastic wave propagation in the ground and to explore the elastic response of buried land mines, a numerical model has been developed.<sup>3,4</sup>

In experimental studies, resonant oscillations have occurred at the location of a buried land mine, when the mine is excited by elastic waves. These resonant effects have been observed for mines of different types, shapes and sizes, including antipersonnel and antitank mines. The resonance significantly enhances the signature of a buried mine and clearly distinguishes it from surrounding clutter objects. In this paper, the resonant behavior of buried antipersonnel mines will be described.

To compute the interaction of elastic waves with a buried land mine on a large scale, a simple model for an antipersonnel mine has been used. Although the model is simple, it predicts resonant oscillations at the location of the buried land mine that are qualitatively very similar to the ones observed in experiments. To investigate the resonant behavior in more detail, a refined mine model has been developed, which more closely resembles the structure of an actual TS-50 antipersonnel mine. The detailed mine model incorporates the parts of the mine which are believed to have an impact on the elastic behavior of the mine. With this model, the characteristics of the resonance can be explored.

In the subsequent section, Sec. 2, the numerical model is explained briefly. In Sec. 3, results obtained with the numerical model are described. First, the interaction of elastic waves with a buried mine is depicted. Then, the resonant behavior of a buried land mine is explained. For this, a parametric study is conducted in which the resonance is studied as a function of the soil properties and the burial depth of the mine.

---

Electronic Mail and Telephone: christoph.schroeder@ece.gatech.edu, 404-894-3123, waymond.scott@ece.gatech.edu, 404-894-3048

## 2. THREE-DIMENSIONAL NUMERICAL MODEL

In the course of the development of the elastic/electromagnetic sensor, experiments have been performed with land mines buried in a large sand-filled box.<sup>1,2</sup> In the experiments, elastic waves are launched by an electrodynamic transducer placed on the surface of the ground. The waves propagate along the surface and interact with the buried land mines. To investigate the characteristics of the elastic wave propagation in the ground, a numerical model has been developed.

### 2.1. Finite-Difference Model

A schematic drawing of the model is shown in Fig. 1 (a). The numerical model is a three-dimensional finite-difference model that computes the elastic wave fields in the time-domain. For the model, the ground is approximated as a linear, isotropic, lossless medium. A first-order formulation in terms of the particle velocity and the mechanical stress is employed. The governing partial-differential equations are discretized by central finite differences, and the characteristic finite-difference grid is introduced. In the finite-difference grid, the field components are not known at the same points in space and time, but they are staggered, as indicated in Fig. 1 (b). The air-ground interface is modeled by a free-surface boundary condition. The solution space is surrounded by a *Perfectly-Matched Layer* (PML) absorbing boundary condition, which absorbs the outward traveling waves and, thus, prevents artificial reflections at the outer grid faces. A detailed description of the numerical model can be found in the literature.<sup>4</sup>

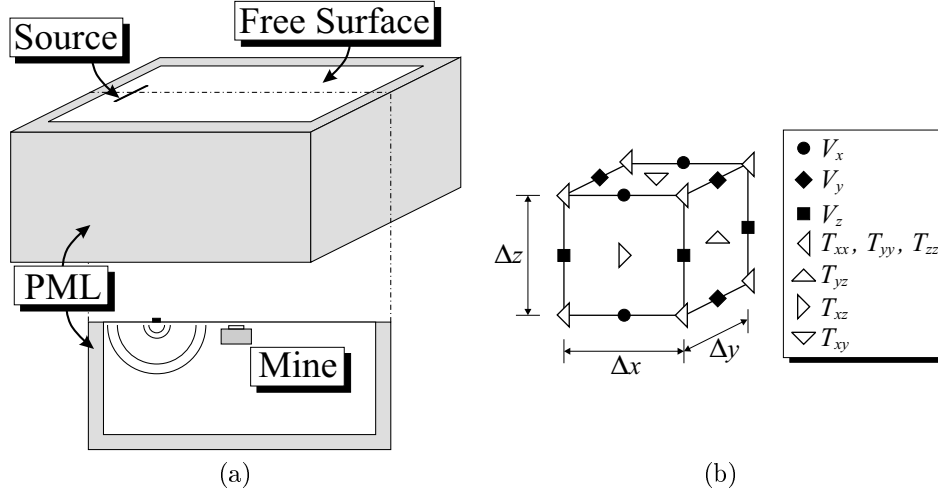


Figure 1. Three-dimensional finite-difference model; (a) lay-out, (b) finite-difference cell.

### 2.2. Material Properties

In the experiments, the mines are buried in a large sand-filled box. If sand is assumed to act in a linear and isotropic manner, its material properties can be described by three independent quantities: the material density  $\rho$ , the pressure wave speed  $c_p$ , and the shear wave speed  $c_s$ . In order to model the sand and its behavior accurately within the numerical model, these quantities have been measured as a function of depth for the sand box used in the experiments.

The material density, the pressure wave speed and the shear wave speed as a function of depth are shown in Fig. 2. All three quantities have been found to be depth dependent. The material density has a value of roughly 1400 kg/m<sup>3</sup> at the surface and increases to about 1600 kg/m<sup>3</sup> at a depth of half a meter. The variation in the material density is due to changes in the water content in the soil. At the surface, the sand is fairly dry. Within the ground, the water content increases steadily, until the water table is reached at a depth of about half a meter. The pressure wave speed and the shear wave speed are both also found to be depth-varying. At the surface, a layer with fairly slow wave speeds exists. Beyond this layer, the pressure wave speed and the shear wave speed increase rapidly. At a depth of half a meter, the pressure wave speed and the shear wave speed have values of 210 m/s and 130 m/s,

respectively.\* The depth variation of the wave speeds is influenced by several mechanisms. The cohesion between the grains of the sand, for example, is affected by the water content, because the water binds the grains of the sand. The cohesion is also altered by the pressure in the ground, which, due to gravity, increases with depth. The increase in the cohesion will cause an increase in the wave speeds. On the other hand, the increase in the material density with depth would, if the stiffness was constant, reduce the wave speeds. It must be noted that, although the measured depth profiles are fairly good approximations of the actual depth profiles in the soil, they are only approximations and the actual depth profile might be more complex.

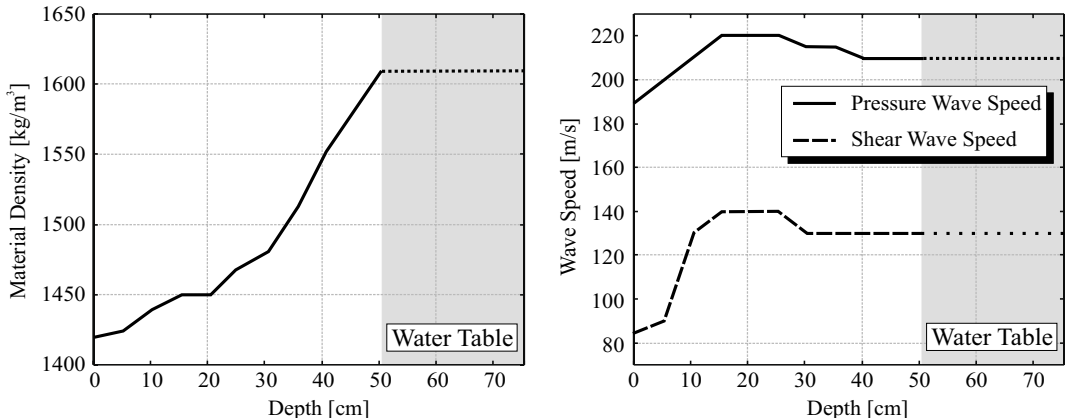


**Figure 2.** The material density and the elastic wave speeds as a function of depth.

### 3. RESULTS

Using the numerical model, the interaction of elastic waves with buried land mines is investigated. First, results are presented that describe the interaction on a large scale using a simple model for the buried mine. Then, the resonant oscillations that are observed at the location of the buried mine are explored by employing a mine model that incorporates many features of an actual mine.

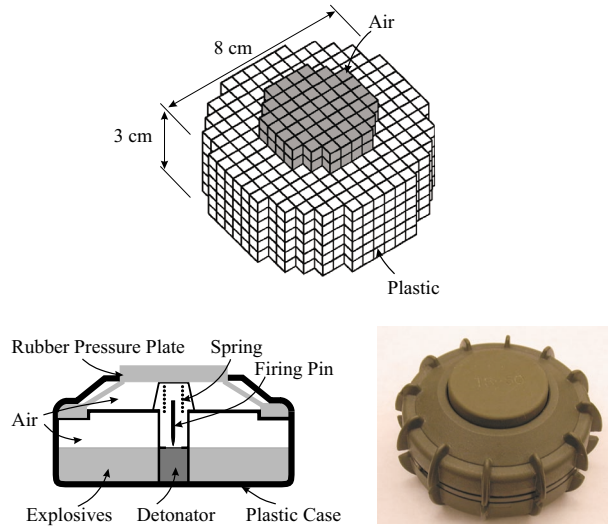
#### 3.1. Interaction of Elastic Waves with a Buried Land Mine

Fig. 3 shows an actual TS-50 antipersonnel mine. Antipersonnel mines are fairly small and have a complex structure. Parts of the mine that might influence its elastic behavior are the explosives, the triggering mechanism, the mine’s case, the rubber pressure plate and the various air chambers. As a first approach, the mine is approximated by a simple model. The simple model has roughly the same dimensions as the TS-50 mine. Due to the cubic structure of the discrete finite-difference grid, the mine is discretized by cubes. The model consists of two parts: a large plastic chamber and a small air-filled chamber on top of the plastic chamber. By inserting the simple mine model into the numerical model, the interaction of elastic waves with a buried mine is computed.

Results are shown in Fig. 4. The interaction of elastic waves with a mine buried 2 cm beneath the surface of the ground is depicted. The vertical particle displacement on the surface plane (top) and on a cross section through the ground (bottom) is shown at four instants in time. A logarithmic color scale is employed, ranging from white (0 dB) to black (-60 dB). The plots describe a surface area of 1.0 m by 0.8 m, and a cross sectional area with a depth of 0.7 m. The source is placed on the surface, to the left of the plots. The distance from the source to the mine is 0.8 m. The excitation is a differentiated Gaussian pulse with a center frequency of 450 Hz.

At the first instant in time,  $T_1$ , a Rayleigh surface wave (R) and a shear wave (S) are seen to propagate. A pressure wave has also been launched, but has already left the range of the plot. On the cross section it is evident

\*The material properties are measured only up to a depth of half a meter and are assumed constant deeper in the ground. This is a vague assumption and probably not true within the water table, but is justifiable, because, within the frequency range of interest, the variation of the material properties deeper in the ground will not have a significant impact onto the wave propagation at and close to the surface.



**Figure 3.** A simple model for a buried antipersonnel mine.

that, due to the variation of the wave speeds in the ground, the shear wave is refracted back towards the surface, and a guided shear wave propagates along the surface. The guided shear wave is ahead of the Rayleigh wave and is clearly visible on the surface. At  $T_2$ , the Rayleigh surface wave just hits the mine. At  $T_3$ , scattered Rayleigh surface waves (rR) and shear waves (rS) can be distinguished. At  $T_4$ , resonant oscillations are visible at the location of the buried mine. Due to the resonant oscillations, the location of the buried mine can be clearly identified on the surface plane. When looking at the wave fields on the cross section, it is evident that the resonant oscillations are confined to the thin soil layer above the mine. It has been shown that, within the numerical model, the resonant oscillations are due to flexural waves coupling into the thin soil layer and forming a pattern of standing waves.<sup>3</sup> A similar resonance has been observed also experimentally for an actual TS-50 mine. For an actual mine, however, the resonant oscillations are due to the soil-mine system, and the resonance is strongly influenced by the resonant behavior of the mine. Thus, for an actual mine the resonant behavior is certainly more complex and cannot be attributed solely to flexural modes in the soil layer above the mine.

### 3.2. Resonance Behavior of a Buried Land Mine

To investigate the resonant oscillations at the location of a buried land mine in detail, a mine model has been developed that closely resembles the structure of an actual mine. The new mine model is shown in Fig. 5. The mine model includes the details of the mine that are believed to have an impact on the mine’s resonant behavior, i. e., the explosives, the plastic case, the rubber pressure plate and the air chambers.

To incorporate the features of an actual mine, a much finer discretization must be chosen for the detailed mine model. Due to limited computer resources, the size of the discretized solution space is reduced to the area immediately surrounding the mine. Because the dimensions of the solution space for this model are small (10 cm by 10 cm by 10 cm), the medium can be approximated as homogeneous. Thus, for all of the following results, the soil properties are assumed constant throughout the solution space.

Results obtained with the detailed mine model are shown in Fig. 6. The vertical particle displacement on the surface plane (top) and on a cross section through the ground (bottom) is shown at four instants in time using the same color scale as earlier. The mine is buried 2 cm beneath the surface. Instead of modeling the transducer on the surface, a vertically polarized plane shear wave is injected from the left. The excitation is a differentiated Gaussian pulse with a center frequency of 1 kHz and, thus, has a wider bandwidth than the excitation used previously. The solution space is surrounded by a PML. For the results in Fig. 6, the material density is chosen to be  $\rho = 1400 \text{ kg/m}^3$ , the pressure wave speed is  $c_p = 250 \text{ m/s}$  and the shear wave speed  $c_s = 80 \text{ m/s}$ . The same values for the pressure wave speed and the material density will be used for all results presented in the following.

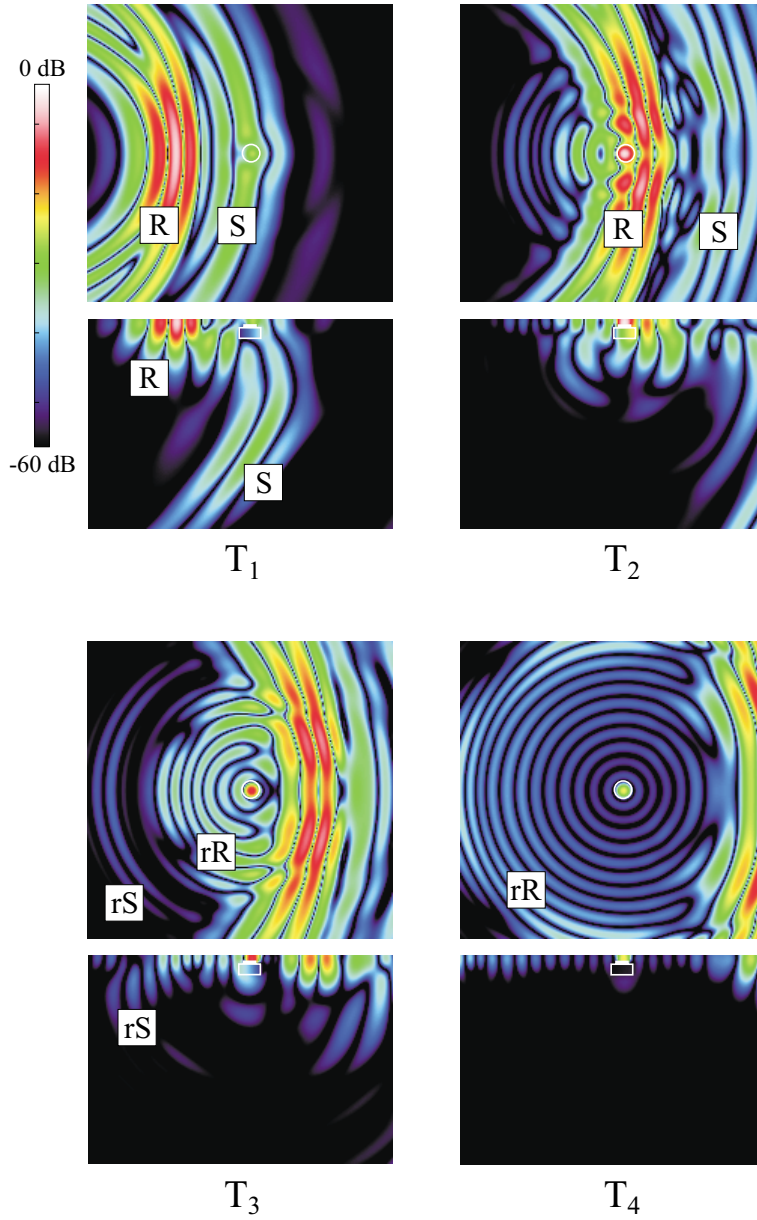


**Figure 4.** Interaction of elastic waves with a buried antipersonnel mine; mine buried 2 cm beneath the surface. The vertical particle displacement on the surface (top) and on a cross section through the ground (bottom) is shown at four instants in time. R: Rayleigh wave; S: shear wave; rR: scattered Rayleigh wave; rS: scattered shear wave.

In Fig. 6, resonant oscillations are seen to be excited at the buried mine. The oscillations appear to be mainly due to the motion of the thin soil layer above the mine and the rubber pressure plate of the mine. The oscillations decay as time progresses. The surface motion seems to be composed of different modes. At  $T_1$  and  $T_3$ , the motion is dominated by a mode describing an upward and downward motion of the surface above the mine. At  $T_4$ , a mode describing a rocking motion of the surface is apparent. A null in the vertical particle displacement along the diameter of the soil layer is clearly visible on the surface and on the cross section. At  $T_2$ , the surface motion seems to be composed of the superposition of at least these two modes.

From the results obtained with the detailed mine model, it becomes clear that the resonance is not only due to flexural modes of the thin soil layer, but rather must be attributed to the resonant behavior of the soil-mine system.

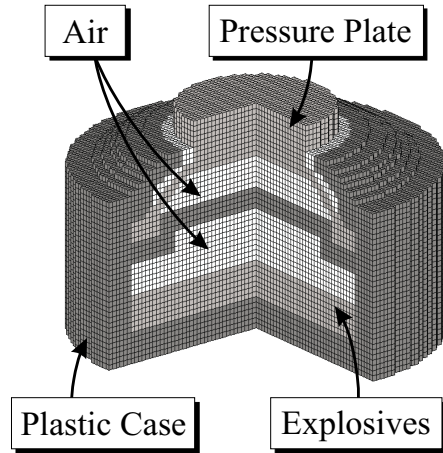


**Figure 5.** Refined mine model that includes details of an actual TS-50 mine such as the explosives, the case, the rubber pressure plate, and the air chambers.

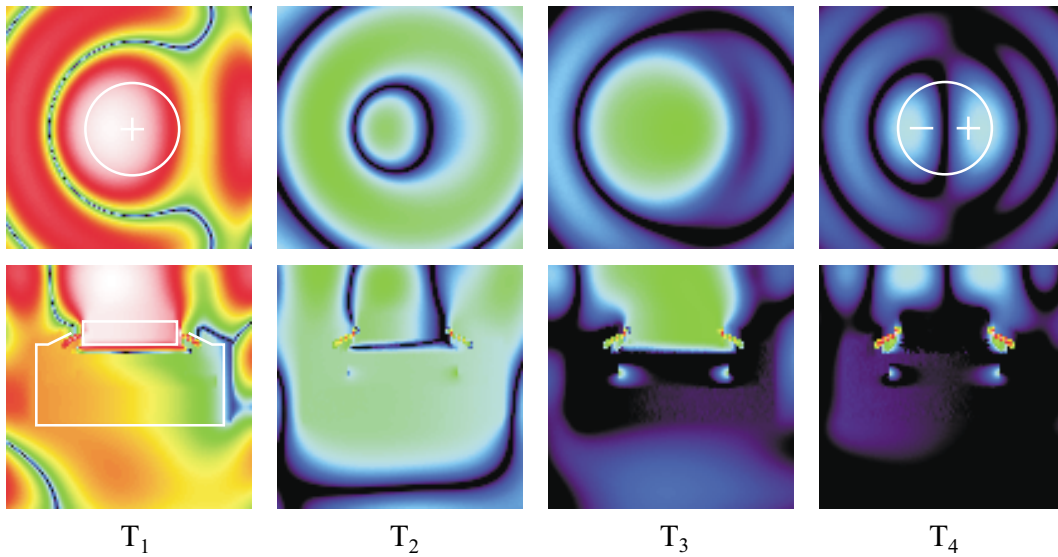


**Figure 6.** Resonant oscillations at the location of a buried land mine; mine buried 2 cm beneath the surface. The vertical particle displacement in the surrounding of the mine as computed with the detailed mine model is shown at four instants in time on the surface plane (top) and on a cross section through the ground (bottom).

The resonant oscillations are caused by the motion of both the soil layer and the rubber pressure plate. This motion will be influenced by various factors. On the one hand, it will strongly depend on the stiffness and thickness of the soil layer above the mine. On the other hand, it will be affected by the mine and its structure. For example, below the rubber pressure plate lies a closed air chamber (see Fig. 5). This air chamber behaves like a spring and has a significant impact on the motion of the pressure plate.

To analyze the resonant behavior at the location of a buried mine in detail, a parametric study of the resonance as a function of the burial depth and the shear wave speed in the ground has been conducted. For this, the vertical motion at one point on the surface above the mine is computed in the time domain. A point is picked that lies 1 cm off the vertical axis of the mine. The motion is Fourier transformed from the time domain into the frequency domain, and, by dividing by the Fourier transform of the incident pulse, the transfer function is determined. From

the transfer function the resonant frequencies of the particle motion can be identified. For the parametric study, shear wave speeds in the range from 40 m/s up to 150 m/s are considered in order to determine the response for fairly loose as well as rather stiff soils. These values are representative for the shear wave speeds at the surface of many common soil types.

Fig. 7 shows the transfer function for a mine buried 1 cm beneath the surface. The shear wave speed in the ground is assumed to be 40 m/s. Below 2.1 kHz, two resonant peaks can be distinguished. The two peaks correspond to two modes of the surface motion. The first mode has a resonant frequency of about 630 Hz and corresponds to an up- and downward motion of the surface. The second mode, at about 1.4 kHz, describes a rocking motion. The behavior of the modes is illustrated in Fig. 7. The two modes that are excited within the soil-mine system are similar in shape to the first two modes of a thin circular disc with clamped edges.<sup>5,6</sup> However, the analogy to the circular disc cannot be used to accurately predict the resonant frequencies of the soil-mine system, because along its edge the soil layer in the model is not rigidly fixed and the structure of the mine has a significant impact on the resonance.

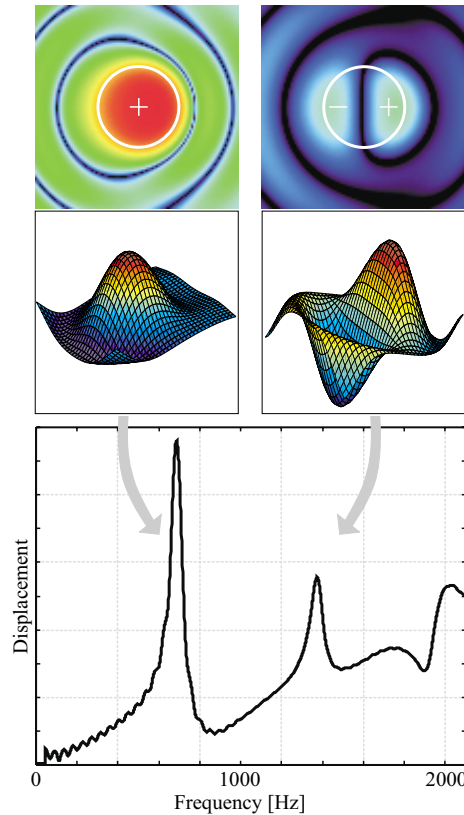


**Figure 7.** Transfer function of a point on the surface above the mine; mine buried at 1cm;  $c_s = 40$  m/s. The two resonant peaks correspond to two modes of the surface motion.

To explore the resonance for mines in different burial scenarios, the resonant behavior is determined as a function of the shear wave speed in the ground and the burial depth of the mine. Fig. 8 shows the transfer function on the left as a function of the shear wave speed in the ground with the burial depth of the mine fixed at 2 cm, and on the right as a function of the burial depth with the shear wave speed kept constant at 40 m/s. It is apparent that the resonant frequencies of the first and second peak are shifted upwards in frequency with increasing shear wave speed. At the same time, their amplitudes drop, and the quality of the resonance is degraded. For increasing burial depth, the resonant frequencies are shifted slightly downwards, and the amplitudes drop drastically. For the mine at 4 cm, the second resonant peak is not distinguishable any more.

To summarize the results, the resonant frequency and the quality factor of the first resonant peak are plotted in

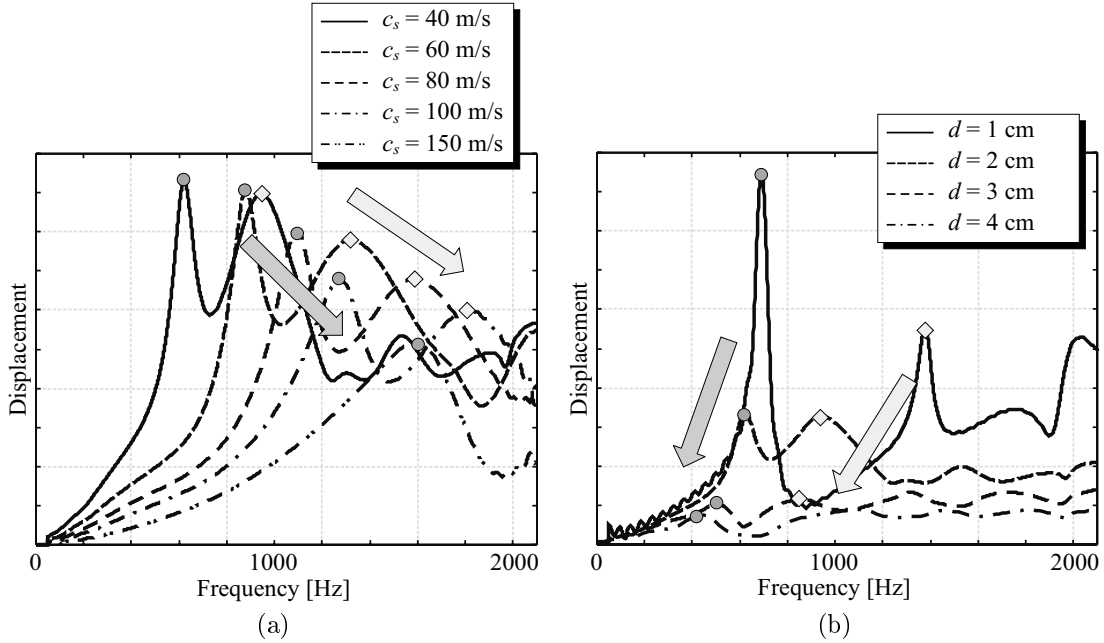


**Figure 8.** Surface motion at a point above the mine in the frequency domain. (a) Mine buried 2 cm beneath the surface, variable shear wave speed; (b) shear wave speed  $c_s = 40$  m/s, variable depth.

two parametric graphs as a function of the shear wave speed in the ground with the burial depth as a parameter. Note that, by varying the shear wave speed in the ground while keeping the material density constant, effectively the stiffness in the ground is being varied. Thus, in these plots the resonant behavior is shown as a function of the stiffness in the ground. In Fig. 9, the resonant frequency and the quality factor are plotted. The top line in each plot corresponds to the mine at a burial depth of 1 cm. Qualitatively, it can be seen that the resonant frequency increases with shear wave speed and decreases with burial depth. The quality factor of the resonance decreases with both shear wave speed and burial depth. The change in the resonant frequency is mainly due to the stiffness in the soil, whereas the change in the quality of the resonance can be attributed to radiation damping. The dominant damping mechanism for the resonance within the model is the radiation of energy into the surrounding soil. The coupling of the thin soil layer above the mine to the surrounding soil increases with the stiffness and the thickness of the layer. Thus, the energy that is radiated also increases, and the damping of the resonance is enhanced.

Resonant oscillations have been observed also experimentally. Fig. 10 shows experimental results obtained with an actual TS-50 mine buried 1 cm beneath the surface. The solid curve indicates the measured transfer function, whereas the dashed gray curve is the transfer function as computed with the numerical model for a mine at 1 cm and with a shear wave speed in the soil of 40 m/s. The curves are seen to be quite different. The second resonant peak in the experimental results is very weak. The authors believe that these differences are mainly due to non-linear effects occurring in the sand. The non-linear effects strongly dampen the high frequency components of the elastic waves and effectively suppress frequency components above about 500 Hz.

#### 4. CONCLUSIONS

If a buried land mine interacts with elastic waves, resonant oscillations are excited at the location of the buried mine. In this paper, these resonant oscillations are explored as a function of burial depth and soil parameters using a numerical model. It has been found that, in general, the resonant behavior is strongly dependent on both the burial depth and the shear wave speed in the soil. The resonant frequency is seen to increase with shear wave speed and to decrease with burial depth. At the same time, the quality factor of the resonance decreases with both shear wave speed and burial depth. The results presented in this paper show conclusively that resonant oscillations do exist at the location of a buried mine for a wide range of different soil types and burial depths.

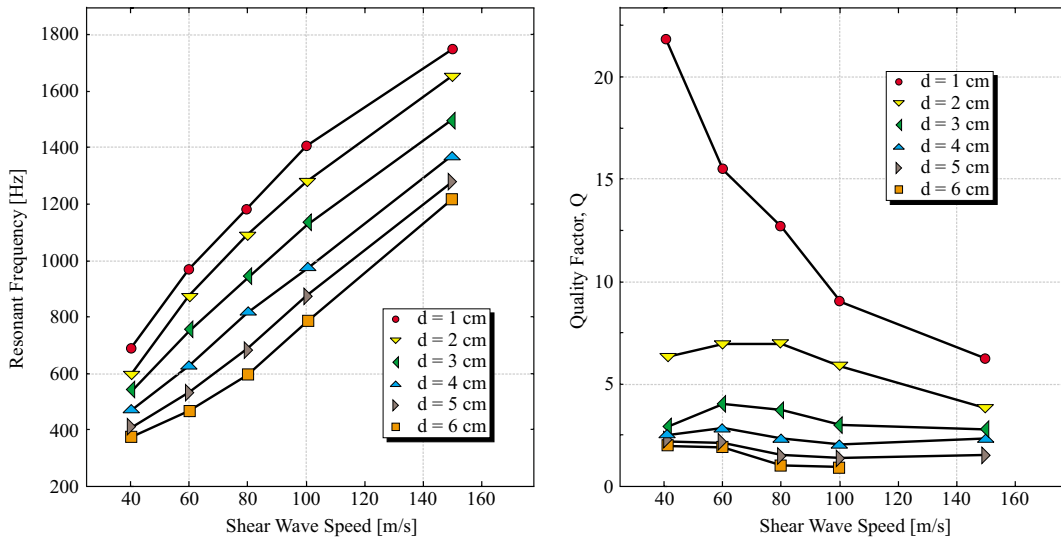


**Figure 9.** Parametric graph of the resonant frequency and the quality factor of the first resonant peak as a function of the shear wave speed in the ground with the burial depth as a parameter.

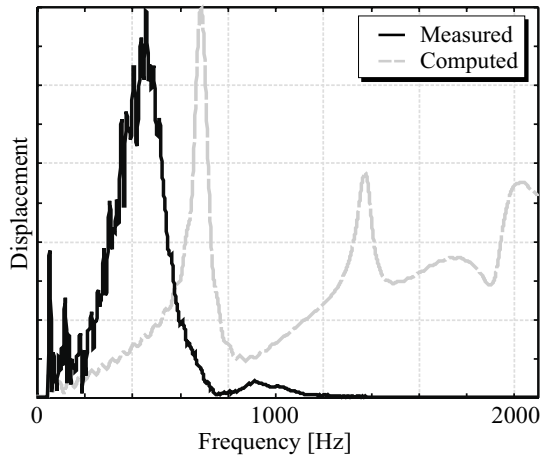


**Figure 10.** Experimental results for a mine buried at 1 cm; transfer function.

### ACKNOWLEDGMENTS

This work is supported in part under the OSD MURI program by the US Army Research Office under contract DAAH04-96-1-0448, by a grant from the US Office of Naval Research under contract N00014-99-1-0995, and by an equipment grant from the Intel Corporation.

### REFERENCES

1. W. R. Scott, Jr., G. D. Larson, and J. S. Martin, "Simultaneous use of elastic and electromagnetic waves for the detection of buried land mines," in *Detection and Remediation Technologies for Mines and Minelike Targets V, Proc. SPIE*, vol. 4038, pp. 667–678, Apr. 2000.
2. W. R. Scott, Jr., J. S. Martin, and G. D. Larson, "Experimental model for a seismic landmine detection system," *IEEE Trans. on Geoscience and Remote Sensing*, to appear July 2001.

3. C. T. Schröder and W. R. Scott, Jr., “A finite-difference model to study the elastic-wave interactions with buried land mines,” *IEEE Trans. on Geoscience and Remote Sensing* **38**, pp. 1505–1512, Jul. 2000.
4. C. T. Schröder and W. R. Scott, Jr., “Three-dimensional FDTD model to study the elastic-wave interaction with buried land mines,” in *Detection and Remediation Technologies for Mines and Minelike Targets V, Proc. SPIE*, vol. 4038, pp. 680–690, Apr. 2000.
5. K. F. Graff, *Wave Motion in Elastic Solids*, Dover Publications, 1975.
6. N. H. Fletcher and T. D. Rossing, *The Physics of Musical Instruments*, Springer-Verlag, New York, 1<sup>st</sup> ed., 1991.